Progress In Electromagnetics Research M, Vol. 108, 163–173, 2022

On-Demand Frequency Switchable Antenna Array Operating at 24.8 and 28 GHz for 5G High-Gain Sensors Applications

Wahaj Abbas Awan[1, *], Mohammad Soruri[2], Mohammad Alibakhshikenari[3, *], and Ernesto Limiti[4]

Abstract—A miniaturized in size linear multiple-input multiple-output (MIMO) antenna array operating on demand at 28 GHz and 24.8 GHz for 5G applications is presented and investigated in this research work. The antenna array has the capability to switch and operate efficiently from 28 GHz to 24.8 GHz with more than 15 dB gain at each frequency, having 2.1 GHz and 1.9 GHz bandwidth, respectively. The unit cell of the proposed antenna array consists of a transmission line (TL) fed circular patch connected with horizontal and vertical stubs. The vertical stubs are used to switch the operating frequency and mitigate the unwanted interaction between the adjacent elements of the antenna array to miniaturize the overall dimension of the array. The proposed antenna array is compared with the recent works published in the literature for 5G applications to demonstrate the features of miniaturization and high gain. The proposed array is a potential candidate for 5G sensors applications like cellular devices, drones, biotelemetry sensors, etc.

1. INTRODUCTION

The demand of wireless electronic devices and interconnecting technologies like the Internet of Things (IoT) and the Internet of vehicles (IoV) have exponentially increased the number of users and congested the allocated unlicensed frequency bands [1]. To meet this demand, an advance in high speed with low latency rate and broad bandwidth communication network, named 5G, is under consideration by the research communities these days [2]. The frequency bands above 24 GHz, i.e., 28, 38, 60, and 73 GHz are among the proposed frequency bands for the 5G, as these are not allocated and available for the unlicensed bands by the Federal Communication Commission (FCC) [3]. The antenna design for the proposed 5G frequency bands is an endeavor for the research groups working in the antenna design in order to keep pace with the advance of research carried out to realize the 5G in other research domains [4-6]. Recently, FCC has finalized the first 5G spectrum auction for the 24 GHz (24.25–24.45, 24.75–25.25) and 28 GHz (27.5–28.35 GHz) and, triggered the researchers to focus their designs at the mentioned bands [7–15].

High propagation losses and non-line-of-sight (NLoS) due to the short wavelength at such high frequencies are the major issues to handle the proposed 5G frequency bands. As far as antenna designing concerns, a MIMO antenna array with high gain is the compensation for propagation losses caused by the high frequency [14–18]. In [11], an 8-element MIMO antenna array operating at 28 GHz is proposed, where 15.6 dBi gain is achieved with an overall dimension of 307.8 mm^3. In [12], a dual-band sectorial

Received 11 December 2021, Accepted 8 February 2022, Scheduled 20 February 2022

* Corresponding author: Mohammad Alibakhshikenari (mohammad.alibakhshikenari@uc3m.es), Wahaj Abbas Awan (wahajabbasawan@ieee.org).

[1] Department of Information and Communication Engineering, Chungbuk National University, Chengju, South Korea. [2] Technical Faculty of Ferdows, University of Birjand, Birjand 9717434765, Iran. [3] Department of Signal Theory and Communications, Universidad Carlos III de Madrid, 28911 Leganés, Madrid, Spain. [4] Electronic Engineering Department, University of Rome "Tor Vergata", Vial Del Politecnico 1, 00133 Rome, Italy.

slotted waveguide antenna array for 28 GHz and 38 GHz is presented with an overall dimension of 3728 mm^3 while the gain is above 12 dB for both resonating frequencies. Parallel and series feeding techniques are used to excite the antenna array in [13, 14]., and the reported gains are 12.15 dBi and 11.9 dBi, with dimensions 228.6 mm^3 and 297 mm^3, respectively. In another work reported in [15], a defected ground structure (DGS) is utilized to enhance the bandwidth of antenna array on tradeoff with larger dimension of 487.6 mm^3 and low gain 10.6 dBi. It has been observed from the recent works that a miniaturized and high gain antenna array operating at multiple frequency bands for the 5G applications is still a challenge for the researchers.

A miniaturized frequency reconfigurable from 28 to 24 GHz MIMO antenna array is presented in this manuscript with an overall dimension of 140.36 mm^3 having gains of 16.02 and 15.07 dB, respectively. MIMO array is based on a compact size novel microstrip patch antenna with operational bandwidths of 2.08 GHz (26.97–29.05 GHz) at 28 GHz and 1.45 GHz (24.12–25.57 GHz) at 24 GHz which covers the FCC proposed bandwidth for the 5G applications [3]. The paper is arranged as follows. The theory and design of the unit cell for the MIMO antenna array are discussed in Section 2. Designing of the linear MIMO antenna array is described in Section 3, and the paper is concluded in Section 4.

2. DESIGN OF THE UNIT ELEMENT OF PROPOSED MIMO ARRAY

2.1. Theory and Design

The schematic of the proposed unit cell for the MIMO antenna array is shown in Fig. 1. A circular patch of radius R is excited with the help of a TL. In order to switch the operating frequency from 28 GHz to 24.8 GHz, the TL fed circular patch is further connected with the symmetric pairs of horizontal and vertical stubs with the help of PIN diodes, as shown in Fig. 1. The addition of the horizontal stubs connected to the circular patch increases and redistributes the amount of current flowing on the surface of the patch which affects the matched impedance of the existing circular patch and results in the shift of operating frequency from 28 GHz along with increase in bandwidth of the radiating patch [19–21], as depicted in Fig. 2. The optimized symmetric vertical stubs are further connected on the edges of the horizontal stubs to control the flow of current density and overall impedance of the patch antenna to radiate at 28 GHz with increased bandwidth, as shown in Fig. 2. The lengths of the vertical stubs are adjusted via PIN diodes to increase the amount of current and match the impedance at 24.8 GHz. So, the switching of PIN diodes from off to on state will shift the operating frequency of the antenna from 28 GHz to 24.8 GHz, the two frequency bands allocated by FCC for the 5G applications.

A thin substrate having a low value of permittivity (ε_r) and loss tangent ($\tan\delta$) is suitable to

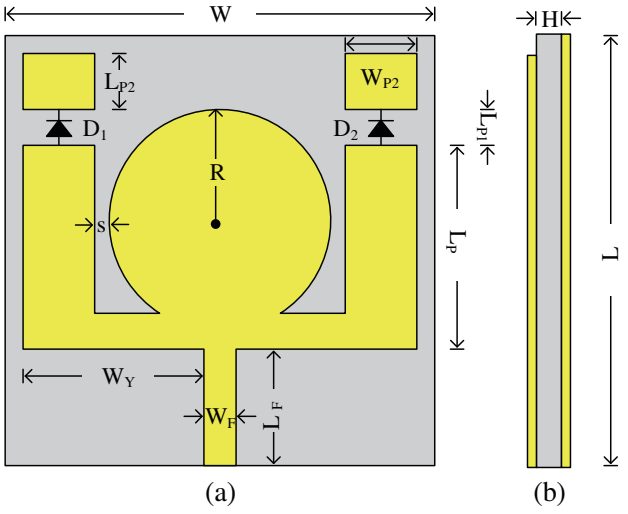

Figure 1. Schematic of the unit cell of proposed MIMO antenna.

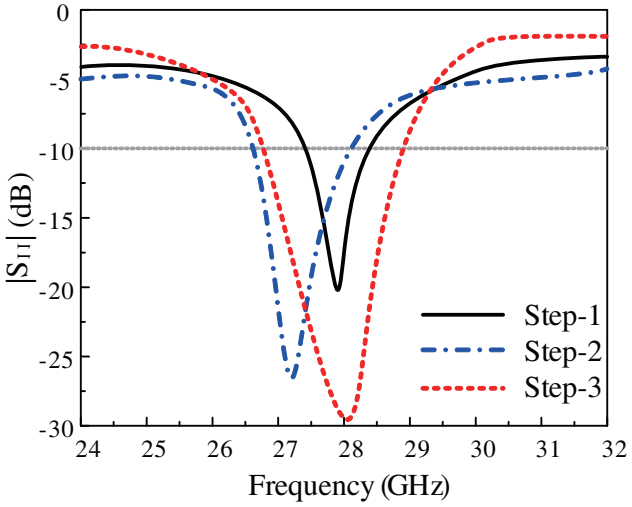

Figure 2. Return loss of various design steps.

radiate at the high frequency for the high gain. A ROGERS RO4350 ($\varepsilon_r = 2.94$, $\tan\delta = 0.0012$) substrate [22] with thickness $H = 0.508\,\text{mm}$ is used to engrave the proposed structure shown in Fig. 1. The radius of the circular patch is calculated by equation [23]. The circular patch is fed by a rectangular TL having the length (L_f) and width (W_f). In order to match the impedance of the circular patch with TL, the optimized values are $L_f = 1.1\,\text{mm}$, $W_f = 0.6\,\text{mm}$, and $R = 1.25\,\text{mm}$. The lengths and widths of the connected symmetric horizontal and vertical stubs are $W_y = 1\,\text{mm}$, $s = 0.2\,\text{mm}$, $L_p = 1.93\,\text{mm}$, $L_{p1} = 0.4\,\text{mm}$, $L_{p2} = 0.27\,\text{mm}$, and $W_p = 0.95\,\text{mm}$, respectively. The bottom side of the substrate is completely grounded having dimensions $L \times W$ ($5\,\text{mm} \times 5\,\text{mm}$).

2.2. Results and Discussion

The proposed geometry of the antenna is simulated in the finite element method (FEM) based high-frequency structure simulator (HFSS) [24], and results are compared by designing a similar antenna in CST Studio Suit. An equivalent model of AlGaAs-Flip-Chip-PIN (PIN) diode with a maximum

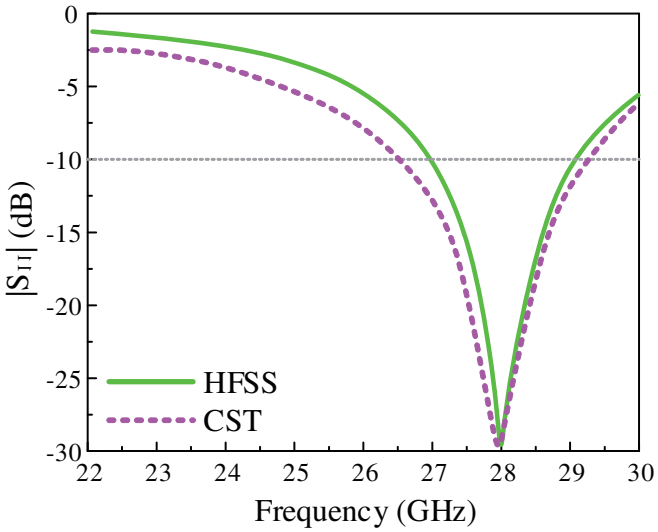

Figure 3. Return loss of unit cell when both diodes are in off state.

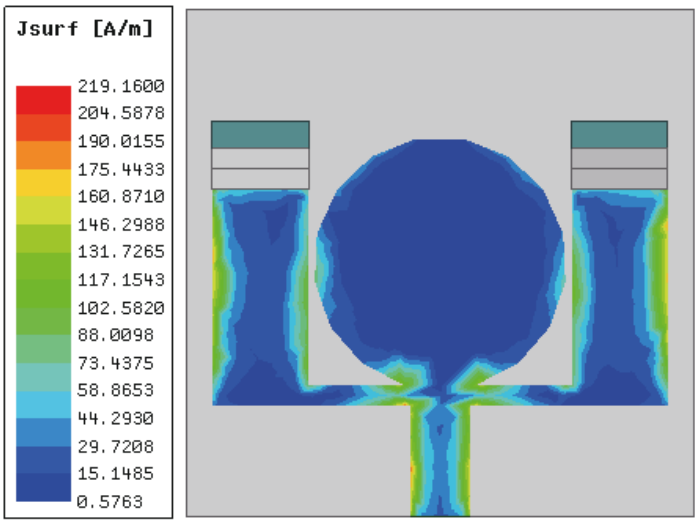

Figure 4. Surface charge distribution at 28 GHz when both diodes are in off state.

operating frequency of 50 GHz [25] is designed in HFSS to switch the operating frequency. Fig. 3 shows the comparison between the results obtained using HFSS and CST for return loss of the simulated antenna when PIN diodes are in off state. The reflection coefficient (S_{11}) shows a promising value of < -30 dB at 28 GHz with a bandwidth of 2.1 GHz, covering the allocated band (28 GHz) for the 5G communication by the FCC. The very low value of S_{11} verifies a good impedance match between feeding and radiating circuitry.

The resultant distribution of current density on the surface of the antenna is shown in Fig. 4. It is noticed that the maximum of the current is distributed on the TL and symmetrical stubs, which demonstrates the feature of currently controlled by them. It is also noticed that the current distribution on the edges of the circular patch and vertical stubs contributes to the increased fringing effect and consequently increases the gain of the antenna. The radiation patterns of the antenna in E- and H-planes at 28 GHz are depicted in Fig. 5, which exhibits a broadside hemisphere high gain of 7 dB with half power beamwidth (HPBW) $\approx 102°$. Fig. 6 shows the co- and cross-components of the polarization in E- and H-planes. The high values of co-components and low values of cross-components in both

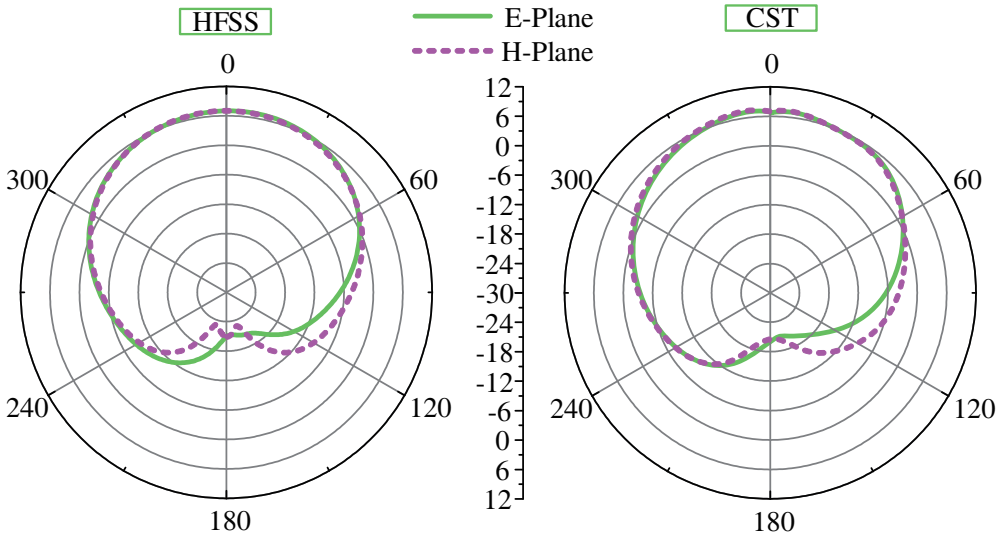

Figure 5. Radiation pattern at 28 GHz when both diodes are in off state.

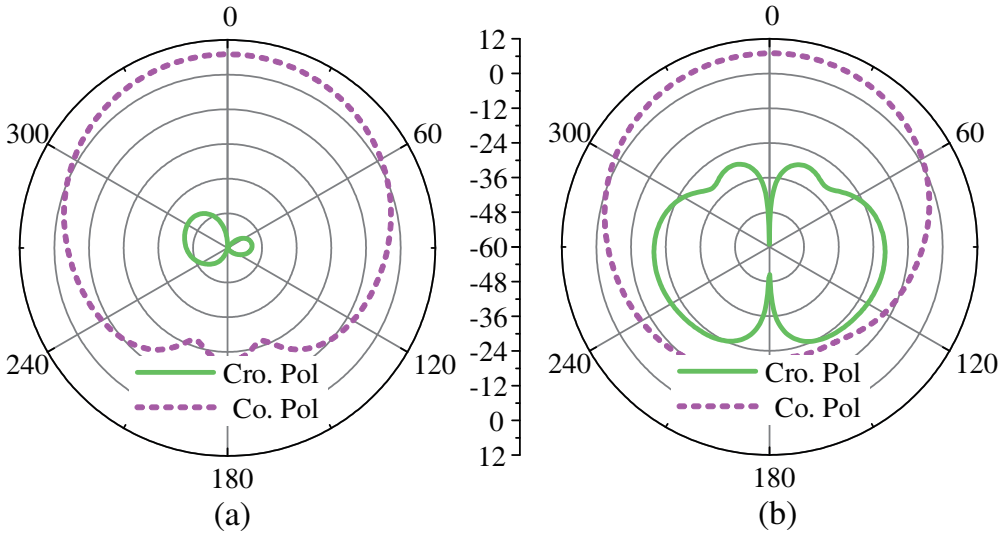

Figure 6. Co-polarization and cross polarization at 28 GHz (a) E-plane (b) H-Plane.

planes characterize the capability of the proposed antenna as a suitable transmitter and/or receiver of the signals at 28 GHz.

Next, the PIN diodes are operated in the ON state while vertical stubs are connected with the patches L_{p1} and L_{p2} via PIN diodes 1 and 2, respectively. The resultant increase in the amount of current density and redistribution on the surface of the antenna due to the increase in physical length of the radiating patch is shown in Fig. 7. The increase in current density increases the electrical length of the antenna, which shifts the operating frequency from 28 GHz to 24.8 GHz. The plot of S_{11} shown in Fig. 8 demonstrates the shift of frequency and resultant impedance matching of the radiation circuitry at 24.8 GHz.

Although the strength of the current density at 24.8 GHz is stronger than at 28 GHz, the current distribution on the edges is less and results in slightly less gain of 6.92 dB with HPBW $\approx 98°$. The broadside hemisphere radiation patterns of the antenna at 24.8 GHz in E- and H-planes are shown in Fig. 9. The co- and cross-components of the antenna at 24.8 GHz to demonstrate the receiving and

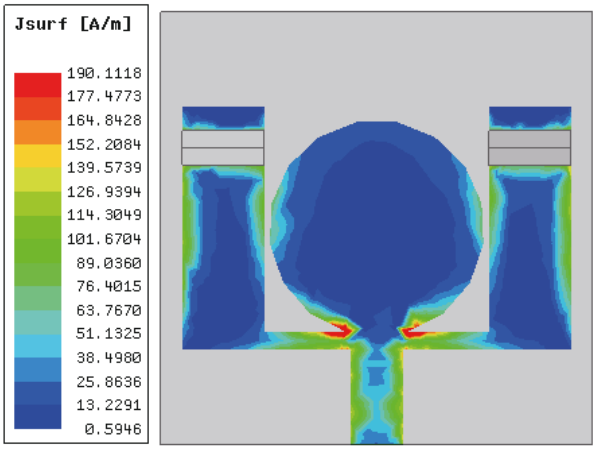

Figure 7. Surface charge distribution at 24.8 GHz when both diodes are in on state.

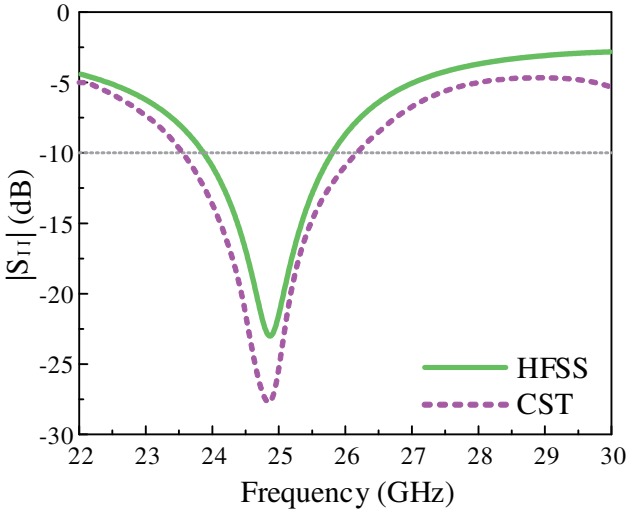

Figure 8. Return loss of unit cell when both diodes are in on state.

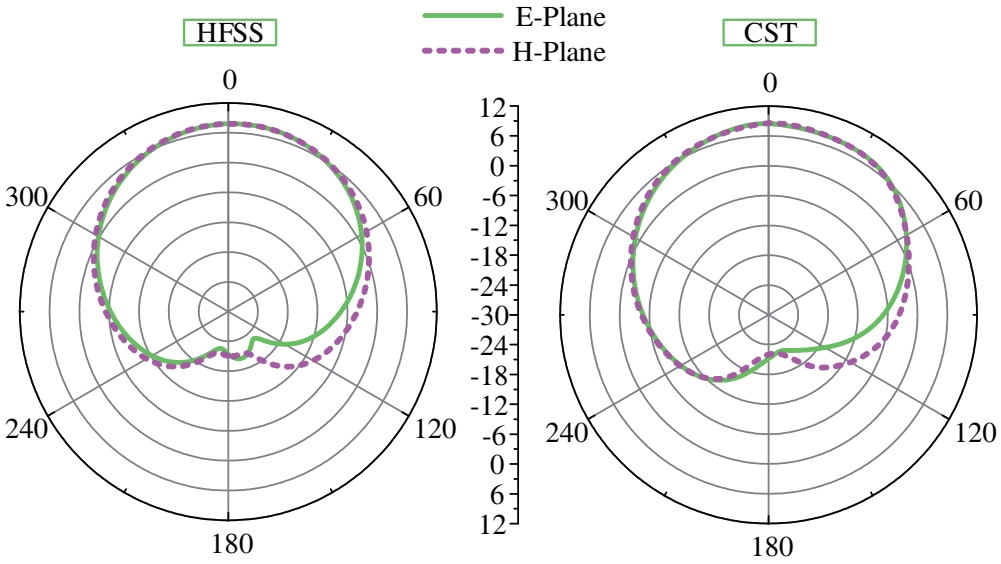

Figure 9. Radiation pattern at 24.8 GHz when both diodes are in on state.

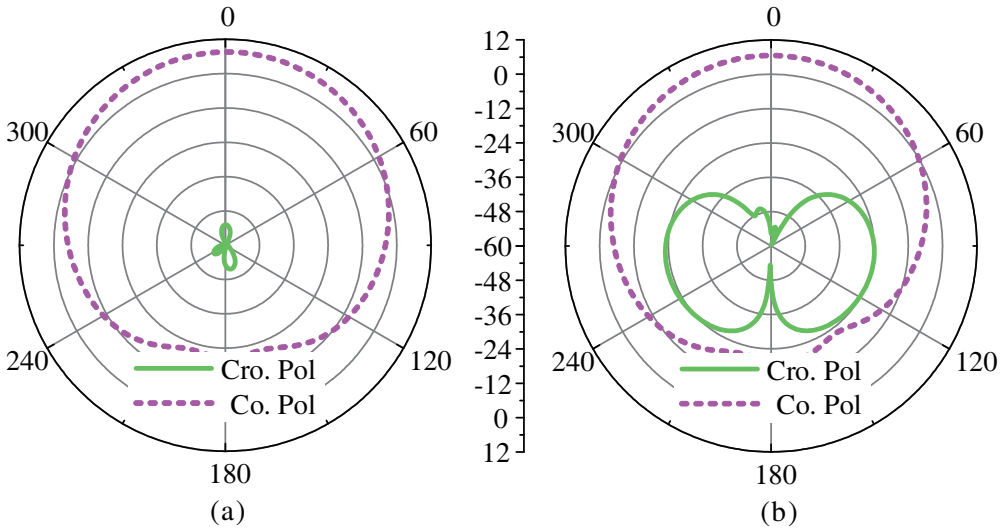

Figure 10. Co-polarization and cross polarization at 24.8 GHz (a) E-plane (b) H-Plane.

rejecting capabilities of the antenna in E- and H-planes are shown in Fig. 10.

Figure 11 presents the input impedance of the proposed antenna. It can be observed from the graphs that the antenna offers a very goof impedance of $\approx 50\,\Omega$ at both resonances for various diode switching states. An increase in impedance matching was observed, which is understandable with respect to the return loss graph shown previously.

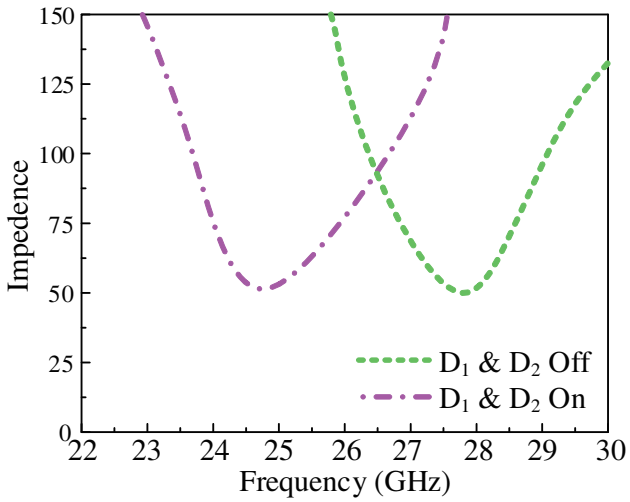

Figure 11. Input impedance of the unit element for both switching states.

3. DESIGN OF LINEAR MIMO ARRAY ANTENNA

In order to design the linear MIMO antenna array, 8 unit cells designed in section 2 are assembled on the RO4350 as shown in Fig. 12. Provided that all the elements in an antenna array are excited with the same phase and magnitude, the separation between the consecutive elements is another critical parameter to control the radiation characteristic and especially the gain of an antenna array. The unwanted interaction between consecutive antenna array elements is the primary factor that does not reduce the distance between elements and places them in close proximity to each other. The presence of stubs is a very useful technique to reduce the unwanted interaction between elements and thus

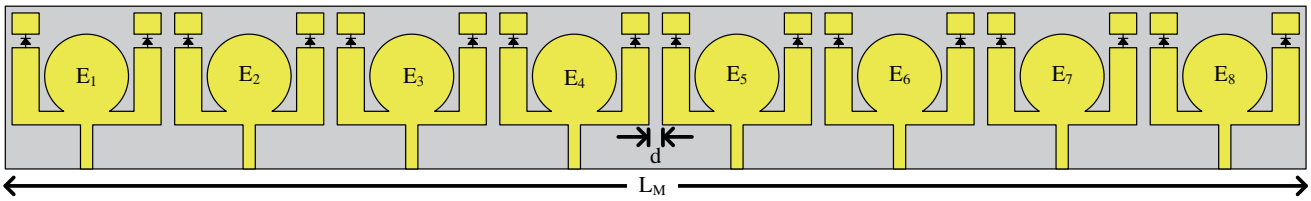

Figure 12. Proposed MIMO antenna array, $d = 2.75$ mm and $L_m = 57.5$ mm.

miniaturize the antenna array [26]. Another benefit of using symmetric vertical stubs in the unit cell is utilized here. The presence of stubs to increase the gain and bandwidth of the unit cell also serves to mitigate the unwanted interaction between the two consecutive elements and consequently reduces the overall size of the proposed array.

The maximum distance between two consecutive elements is kept at $\lambda/4$ instead of conventional distance $\lambda/2$ [23], where λ is the free space wavelength at 28 GHz. Fig. 13 shows S_{ii} and S_{ij}, where $i = j = 1, 2, \ldots 8$, results of the 8 element linear MIMO antenna array when all diodes are in OFF state. It is noticed that the isolation enhancement between two consecutive elements is less than -17 dB at 28 GHz. Fig. 14 shows the gain of the proposed MIMO antenna array in E- and H-planes at 28 GHz. The high gain of 16.02 dB is observed in both E- and H-planes at the central frequency of 28 GHz, which demonstrates the reduction of unwanted interaction between antenna elements in the near field region and in phase constructive interference of radiated fields by individual antenna elements in far field region. Moreover, Fig. 14 shows the fan beam radiation pattern, a wide beam in one plane and a pencil beam in the other plane with the same magnitude. The proposed array demonstrates a hemisphere broadband pattern in E-plan while a pencil beam in H-plane. Fan beam is another required feature and high gain, wideband, and beam steering characteristic for the 5G applications [18].

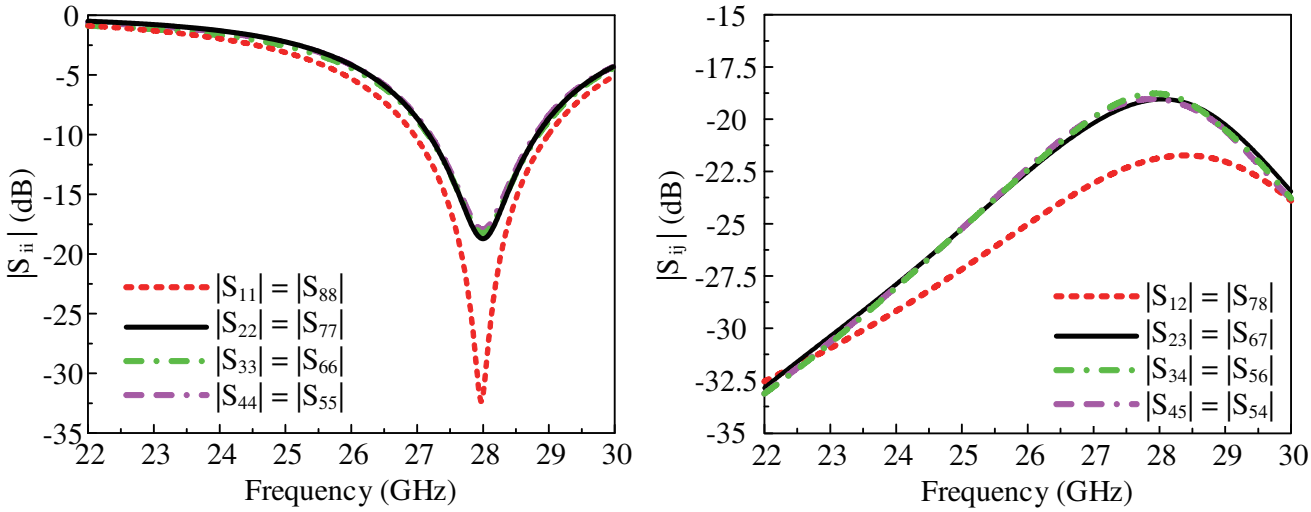

Figure 13. S-Parameter of proposed MIMO array when both diodes are in off state.

Next, the linear MIMO antenna array is simulated with all the PIN diodes in ON mode to switch the operating frequency of the array from 28 GHz to 24.8 GHz. Although the array is operated at 24.8 GHz, with PIN diodes in ON state, the physical separation between any two consecutive elements is still $\lambda/4$, where λ is the free space wavelength at 28 GHz. It means that the electrical distance between two consecutive antenna elements is slightly greater than $\lambda_1/4$, where λ_1 is the free space wavelength at 24.8 GHz. The resultant S_{ii} and S_{ij} parameters are shown in Fig. 15, which shows the improved isolation enhancement between two consecutive antenna elements. Fig. 16 shows the radiation pattern of the linear MIMO antenna array at 24.8 GHz in E- and H-planes. A fan beam radiation pattern with

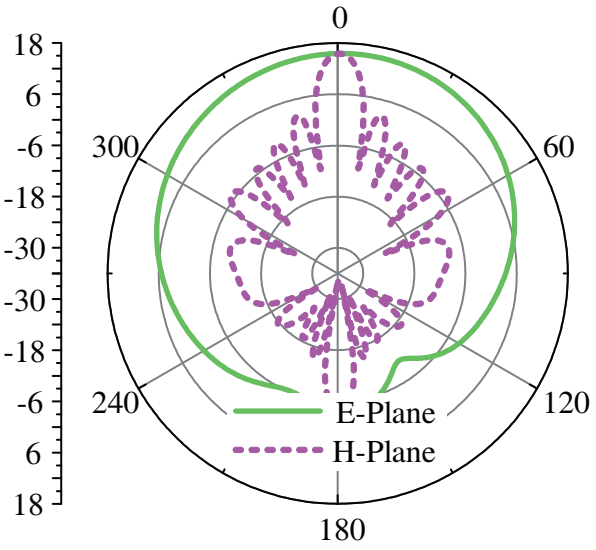

Figure 14. Radiation pattern of proposed MIMO array at 28 GHz when both diodes are in off state.

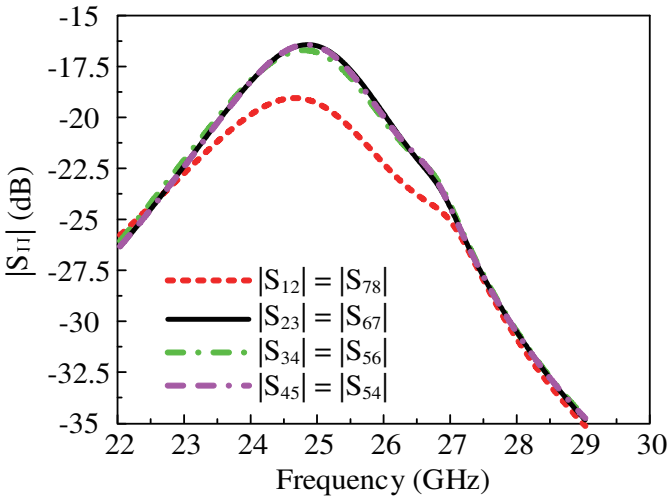

Figure 15. *S*-Parameter of proposed MIMO array when both diodes are in on state.

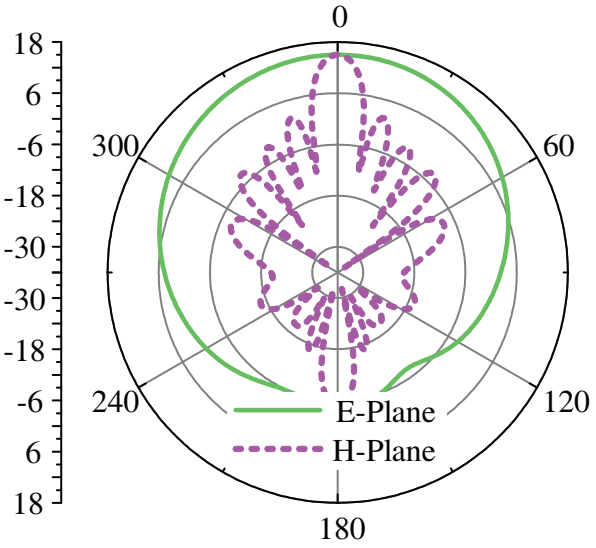

Figure 16. Radiation pattern of proposed MIMO array at 24.8 GHz when both diodes are in on state.

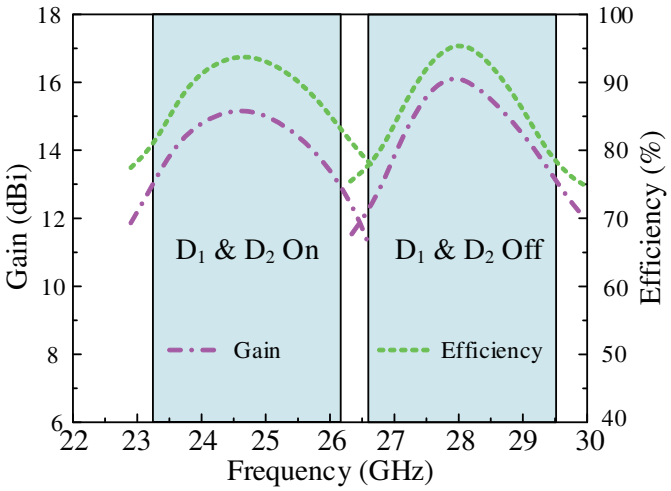

Figure 17. Gain and efficiency plot of the proposed MIMO antenna array.

the gain of 15.07 dB is observed.

Figure 17 depicts the gain and efficiency of proposed MIMO antenna array for both diodes in On- and Off-states. It can be observed that in both states of diode the gain > 14 dBi in operational region along with radiation efficiency of $> 80\%$, as illustrated in Fig. 17.

Envelope Correlation Coefficient (ECC), being a fundamental component to examine the MIMO functionality of the antenna, is studied here. Ideally, the ECC value should be zero. However, in the actual case, due to various losses, the ECC < 0.5 is acceptable. For any MIMO antenna system, the ECC can be calculated using the formula given in [27].

$$\mathrm{ECC}(1,i) = \frac{|S_{11}^{*}S_{1i} + S_{i1}^{*}S_{ii}|}{(1-|S_{11}|^2-|S_{i1}|^2)(1-|S_{ii}|^2-|S_{1i}|^2)} \tag{1}$$

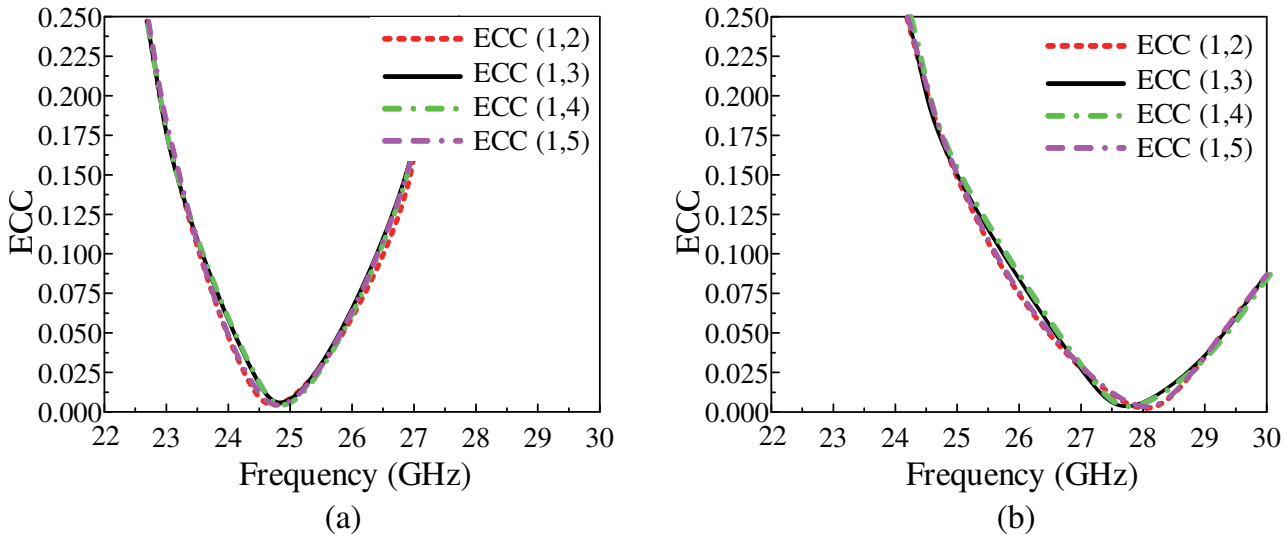

Figure 18. Simulated ECC graphs of the proposed antenna (a) D_1 and D_2 is in On-state (b) D_1 and D_2 is in Off-state.

here i represents the number of the elements with respect to which ECC was calculated. It can be observed from Fig. 18 that for both diodes, either in On- or in Off-state, the ECC value was reported to be less 0.75 in the operational region. Thus, the presented work offers a very low ECC making it a suitable candidate for MIMO applications as well.

4. FABRICATION AND MEASUREMENT CHALLENGES

The antenna was initially simulated using Electromagnetic Solver HFSS, and afterward a similar antenna was designed in CST to analyze the result, as shown in previous Sections 2 and 3. Considering a realistic scenario, instead of using simple copper and slot configuration, an equivalent model of the AlGaAs-Flip-Chip-PIN diode, having a maximum operating frequency of 50 GHz, was made using lumped elements in both simulators. The antenna offers very close results in two different Electromagnetic Solvers, which works using different algorithms. Thus, based upon these validations, it can be said that with low tolerance fabrication, a similar result can be obtained by measurements. Moreover, parametric analysis was performed on various parameters of the antenna to find the minimum acceptable tolerance. It was observed during the investigations that the antenna offers a fabrication tolerance of > 0.01 mm. It means that a highly accurate fabrication setup may be required to fabricate the antenna having a tolerance of > 0.01 mm. Hence the chemical etching or photo-electric etching scheme will not work for the proposed work. Therefore, considering the challenges mentioned above using fabrication techniques with high precision levels, measured results can be obtained close to the simulated one.

5. COMPARISON WITH STATE-OF-THE-ART-WORK

Table 1 shows the comparison of the proposed MIMO antenna array with recent antenna arrays proposed for the 5G applications operating at multiple frequencies. The proposed antenna array achieved the miniaturization of 38.6%–96.23%, with a comparatively high gain of > 15.0 dB. Last, with an overall compact dimension of $5 \times 57.5 \times 0.508\,\text{mm}^3$, the proposed array is a potential candidate for the 5G applications requiring compact size like cellular devices, PC tablets, drones, biotelemetry sensors, etc. Specifically, the width $W_m = 57.5$ mm of the array fits in the commercially available cellular devices well having a width of around 65 mm.

Table 1. Comparison of proposed work with recent works.

Reference No.	Dimension (mm^3)	Miniaturization achieved	Max Gain (dB)
[11]	307.8	54.4%	15.6
[12]	3728	96.23%	15.6
[13]	228.6	38.6%	12.15
[14]	297	52.73%	11.5
[15]	487.68	71.22%	10.6
Proposed Work	140.36	——	16.02

6. CONCLUSION

An on-demand frequency switchable, high gain, and miniaturized linear MIMO antenna array operating at 28 GHz and 24.8 GHz is presented and investigated in this paper. It is demonstrated that the pairs of symmetric vertical and horizontal stubs are used to control the amount of current on the radiating patch, thus switch the frequency and enhance the gain of the unit cell proposed for the MIMO antenna array. Vertical stubs are used to minimize the unwanted interaction between the adjacent antenna elements so that the placement of the antenna elements in close proximity is feasible, and the feature of miniaturization is attained. The vertical stubs are also used to switch the operating frequency from 28 GHz to 24.8 GHz with gains of 16.02 dB and 15.07 dB, respectively. Based on high gain capabilities, broad bandwidth, fan beam radiation pattern, frequency reconfigurability, and miniaturized size, the linear MIMO antenna array is proposed as a suitable candidate for 5G applications like cellular devices, PC tablets, drones, biotelemetry devices, etc.

ACKNOWLEDGMENT

This project has received funding from Universidad Carlos III de Madrid and the European Union's Horizon 2020 research and innovation program under the Marie Sklodowska-Curie Grant 801538. In addition, the authors appreciate the partial support from the Antenna and Wireless Propagation Group (https://sites.google.com/view/awpgrp/home).

REFERENCES

1. Andrews, J. G., S. Buzzi, W. Choi, et al., "What will 5G be?" *IEEE J. Sel. Areas Commun.*, Vol. 32, No. 6, 1065–1082, 2014.
2. Naqvi, A. H. and S. Lim, "Review of recent phased arrays for millimeter-wave wireless communication," *Sensors*, Vol. 18, No. 10, 3194, 2018.
3. Federal Communications Commission (FCC), FCC Establishes Procedures for First 5G Spectrum Auctions, Aug. 2018.
4. Yang, B., Z. Yu, J. Lan, R. Zhang, J. Zhou, and W. Hong, "Digital beamforming-based massive MIMO transceiver for 5G millimeter-wave communications," *IEEE Trans. Microw. Theory Tech.*, 1–16, 2018.
5. Rappaport, T. S.; S. Sun, R. Mayzus, H. Zhao, Y. Azar, K. Wang, G. N. Wong, J. K. Schulz, M. Samimi, and F. Gutierrez, "Millimeter wave mobile communications for 5G cellular: It will work!" *IEEE Access*, Vol. 1, 335–349, 2013.
6. Dehos, C., J. González, A. Domenico, D. Kténas, and L. Dussopt, "Millimeter-wave access and backhauling: The solution to the exponential data traffic increase in 5G mobile communications systems?" *IEEE Commun. Mag.*, Vol. 52, 88–95, 2014.

7. Jamaluddin, M. H., M. Kamarudin, and M. Khalily, "Rectangular dielectric resonator antenna array for 28 GHz applications," *Progress in Electromagnetics Research*, Vol. 63, 53–61, 2016.
8. Yashchyshyn, Y., K. Derzakowski, O. Bogdan, et al., "28 GHz switched-beam antenna based on S-PIN diodes for 5G mobile communications," *IEEE Antennas Wirel. Propag. Lett.*, Vol. 17, No. 2, 225–228, , 2018.
9. Bang, J., J. Choi., et al., "A SAR reduced MM-wave beam-steerable array antenna with dual-mode operation for fully metal-covered 5g cellular handsets," *IEEE Antennas Wirel. Propag. Lett.*, 2018.
10. Li, W. T., M. Wei, B. Badamchi, H. Subbaraman, and X. Shi, "A novel tri-band reconfigurable microstrip patch antenna," *Frequenz*, Vol. 74, No. 7–8, 247–253, 2020.
11. Yu, B., K. Yang, C.-Y.-D. Sim, et al., "A novel 28 GHz beam steering array for 5G mobile device with metallic casing application," *IEEE Trans. Antennas Propag.*, Vol. 66, No. 1, 462–466, 2018.
12. Sodré, Jr., A. C., I. F. da Costa, R. A. dos Santos, H. R. D. Filgueiras, and D. H. Spadoti, "Waveguide-based antenna arrays for 5G networks," *International Journal of Antennas and Propagation*, Vol. 2018, Article ID 5472045, 10 pages, 2018.
13. Ullah, H. and F. A. Tahir, "A broadband wire hexagon antenna array for future 5G communications in 28 GHz band," *Microw. Opt. Technol. Lett.*, 1–6, 2018.
14. Mao, C., M. Khalily, P. Xiao, T. W. C. Brown, and S. Gao, "Planar sub-millimeter-wave array antenna with enhanced gain and reduced sidelobes for 5G broadcast applications," *IEEE Trans. Antennas Propag.*, Vol. 67, No. 1, 160–168, Jan. 2019.
15. Jilani, S. F., A. Alomainy, et al., 'Millimetre-wave T-shaped MIMO antenna with defected ground structures for 5G cellular networks," *IET Microw. Antennas Propag.*, Vol. 12, No. 5. 672–677, 2018.
16. Zhang, J., X. Ge, Q. Li, M. Guizani, and Y. Zhang, "5G millimeter-wave antenna array: Design and challenges," *IEEE Wirel. Commun.*, Vol. 24, 106–112, 2017.
17. Hong, W., K.-H. Baek, Y. Lee, et al., 'Study and prototyping of practically large-scale mmWave antenna systems for 5G cellular devices," *IEEE Commun. Mag.*, Vol. 52, No. 9, 63–69, 2014.
18. Roh, W., J. Y. Seol, J. H. Park, et al., 'Millimeter-wave beamforming as an enabling technology for 5G cellular communications: Theoretical feasibility and prototype results," *IEEE Commun. Mag.*, Vol. 52, No. 2, 106–113, 2014.
19. Naqvi, S. A. and M. S. Khan, "Design of a miniaturized frequency reconfigurable antenna for rectenna in WiMAX and ISM frequency bands," *Microw. Opt. Technol. Lett.*, Vol. 60, 325–330, 2018.
20. Awan, W. A., A. Zaidi, N. Hussain, A. Iqbal, and A. Baghdad, "Stub loaded, low profile UWB antenna with independently controllable notch-bands," *Microw. Opt. Technol. Lett.*, 1–8, 2019.
21. Naqvi, S. A., "Miniaturized triple band and ultra-wideband (UWB) fractal antennas for UWB applications," *Microw. Opt. Technol. Lett.*, Vol. 59, 1542—-1546, 2017.
22. "Rogers Corporation", www.rogerscorp.com, accessed Feburary 2021.
23. Balanis, C. A., *Antenna Theory-Analysis and Design*, Wiley, 1997.
24. Ansys HFSS, ver. 2016.2, Ansys Corporation, Pittsburgh, PA, 2017.
25. "MACOM", www.macom.com, accessed Feburary 2021.
26. Ta, S. X., H. Choo, and I. Park, "Broadband printed-dipole antenna and its arrays for 5G applications," *IEEE Antennas and Wireless Propagation Letters*, Vol. 16, 2183–2186, 2017.
27. Hussain, N., et al., "Compact wideband patch antenna and its MIMO configuration for 28 GHz applications," *AEU-International Journal of Electronics and Communications*, Vol. 132, e153612, 2021.